Cavitating Flow in Coaxial Injector of Liquid-Fueled Rocket Engine

Takao Inamura
Hirosaki University, Hirosaki, Japan
Masatoshi Daikoku
Hachinohe Institute of Technology
Yoshio Nunome, Takuo Onodera, Hiroshi Sakamoto, Akinaga Kumakawa
and Hiroshi Tamura
Japan Aerospace Exploration Agency

Introduction

The atomization characteristics, such as droplet diameter, spray penetration, spray concentration, etc. are some of the most important parameters for a liquid-fueled rocket engine[1]. The spray characteristics affect not only the combustion efficiency, but also the combustion instability. The oscillation of the atomization of a propellant is one of the causes of the combustion instability[2]. The fluctuation of the atomization oscillates the heat release by the combustion, and then the thrust of the engine. Thus, the coupling of the fluctuations of the atomization and the heat release excites and sustains the combustion instability. So, to understand the details of the atomization phenomena is very important to increase the overall efficiency of the engine and to reduce the combustion instability.

In the present study, we focused the atomization phenomena of a coaxial injector widely used in the liquid-fueled rocket engine. Specially, we investigated the cavitating flow in the coaxial injector in detail, because the behavior of the cavitation bubbles in the injector affects greatly the spray characteristics and causes the fluctuation of the atomization[3,4].

Experimental Apparatus and Conditions

The experimental setup used in the present report is shown in Fig.1. The test chamber is a cylindrical type with an inner diameter of 400 mm and length of 1500 mm, and can be pressurized by the high-pressure air up to 1 MPa. The chamber has four glass windows on two diagonal lines for the optical access. These two diagonal lines meet at right angles. The still photographs and movies of the cavitating flow were taken by the still camera and high-speed video camera through the glass windows, respectively. As the light sources of photograph and movie, the strobe light was used for the still photograph and the spot light for the movie.

The water was pressurized by the high-pressure air in the water tank. The water was supplied from the water tank to the test chamber through the electromagnetic valve and the flowrate control valve. The water flowrate was measured by the turbine flowmeter.

In the present study, we used the injector with the rectangular cross section and an orifice depicted in Fig.2. We used the injector with the rectangular cross section, because of easy observation of a liquid flow in the injector. The injector is made of transparent acrylic resin for the optical access. The dimensions of the injectors were determined on the basis of a rocket engine injector. The pressure in the plenum chamber of the injector was measured by the pressure gauge. The pressure tap is drilled on the side wall just upstream of the entrance of the contraction section as shown in Fig.2. The oscillation of the injector was measured by the acceleration sensor glued on the side wall of the injector.

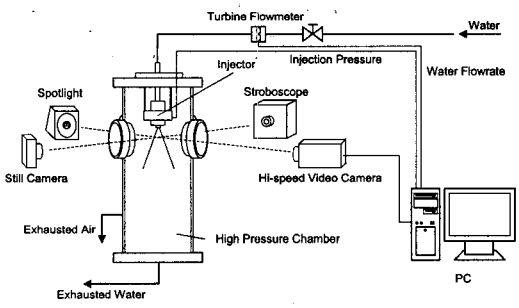

Fig.1 Experimental apparatus

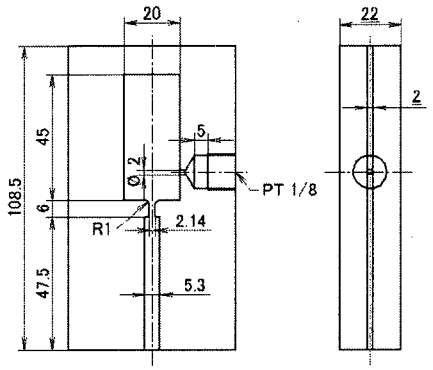

Fig.2 Injector

Table 1 Experimental conditions

Liquid	Water
Injection Pressure, Pi (MPa)	0.2 — 1.2
Back Pressure, Pb (MPa)	0.1 — 0.5
Reynolds Number, Re	30000 — 75000

The pressure gauge and the acceleration sensor attached on the injector, the still camera, video camera and the electromagnetic valve were connected to the computer. They are controlled by the LabVIEW software developed by National Instruments, and the time evolution data of the pressure and the acceleration, and the pictures of the still camera and the video camera were stored in the computer.

As the test liquid, the tap water was employed in the present experiments. The tap water was supplied in the water tank one hour before the test start, and the special evacuating operation was not performed. The experimental conditions are shown in Table 1. The Reynolds number, Re and the

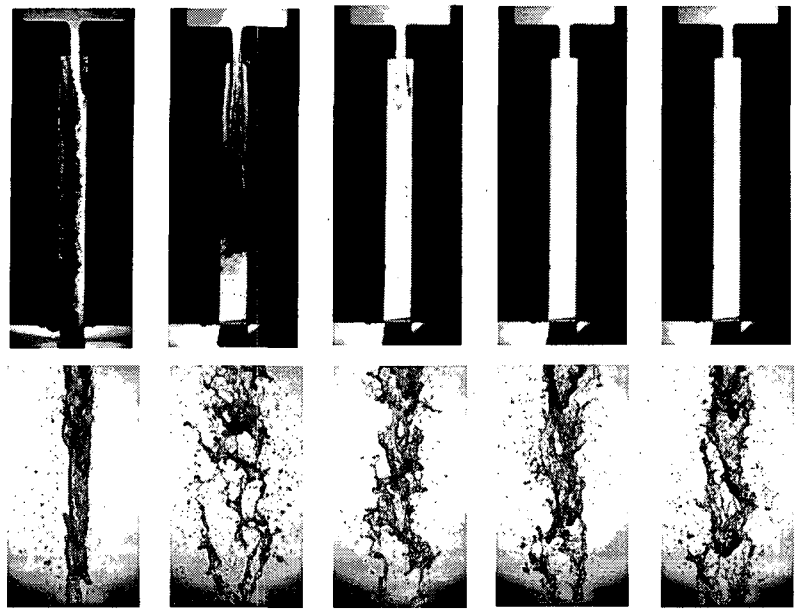

Pb=0.1MPa	0.2	0.3	0.4	0.5
Pi=0.704MPa	0.698	0.707	0.810	0.907
K=0.192	0.379	0.569	0.754	0.929

Fig.3 Cavitating flow in injector

cavitation number, K are defined by the following equations, respectively:

$$\mathrm{Re} = \frac{V \cdot W}{\upsilon} \tag{1}$$

$$\mathrm{K} = \frac{P_b - P_v}{\frac{1}{2}\rho V^2} \tag{2}$$

where, V, W, P_b and P_v indicate the average water velocity in the contraction section, the width of the contraction section (=2.14 mm), the back pressure in the test chamber and the water vapor pressure, respectively. ρ and ν indicate the density and kinetic viscosity of the water, respectively. V was calculated from the water flowrate and the cross sectional area of the contraction section.

Experimental Results and Discussions

Figure 3 shows the cavitating flow in the injector and the disintegration phenomena of a liquid jet 150 mm downstream of the injector exit. The cavitation number changes from 0.192 to 0.929 at constant Reynolds number of 68000. At P_b=0.1 MPa cavitation bubbles reach the injector exit. The cavitation bubbles flow the left side of a liquid flow passage, and the right side is filled with the water. By the observations, the water always adheres to the left side or right side of the passage, and never separates simultaneously from the both side walls. From the photographs of the disintegration phenomena, the atomization of a water jet is clearly poor compared to the other injection conditions. At P_b=0.2 MPa the cavitation bubbles collapse upstream of the injector exit, and the atomization is improved greatly. At

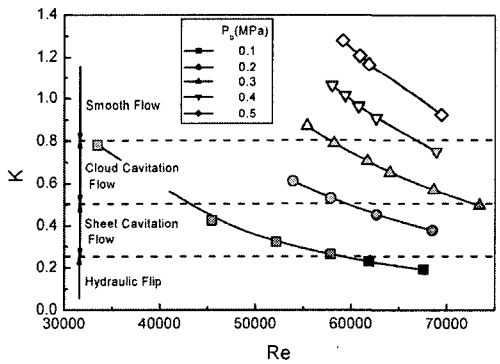

Fig.4 Classification of cavitating flow

P_b=0.3 MPa the cavitation bubbles occur near the entrance of the contraction section, and then collapse immediately. In this condition the atomization gets worse. At P_b=0.4 and 0.5 MPa the cavitation inception is no longer observed from the photographs.

Figure 4 classifies the cavitating flow pattern versus the Reynolds number and cavitation number. Under the constant back pressure, the cavitation number decreases monotonously with an increase of the Reynolds number. This is because that under the constant back pressure the cavitation number is inversely proportional to the square of the Reynolds number, as derived from Eqs.(1) and (2). From the figure, it is clear that the pattern can be classified by only the cavitation number for all back pressure and Reynolds number conditions, as follows:

K<0.25 Hydraulic Flip
0.25<k<0.5 Sheet Cavitation Flow

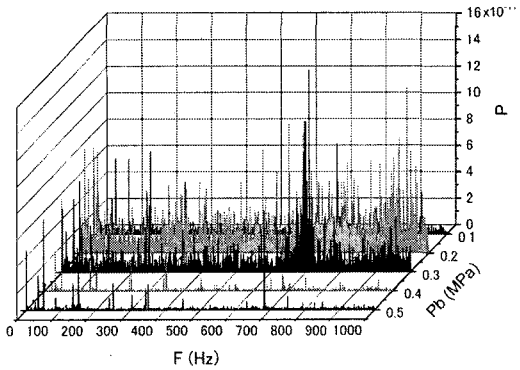

Fig.5 FFT analysis of injector oscillation

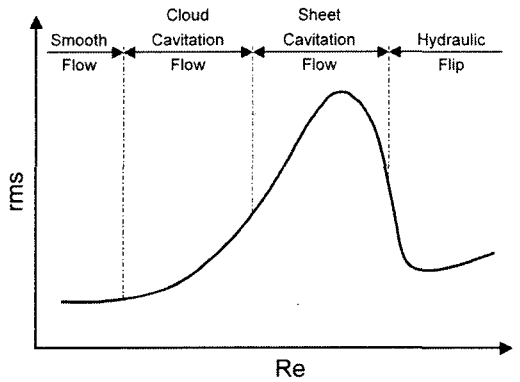

Fig.6 Relationship between injector oscillation and Re

0.5<K<0.8 Cloud Cavitation Flow
K>0.8 Smooth Flow

The time evolutions of the acceleration of the injector measured by the acceleration sensor were analyzed by the FFT analyzer. Figure 5 shows the results of the frequency analysis by FFT at Re=68000. The power spectrum versus frequency is depicted for the three back pressures. The peak of the power spectrum near 680 Hz corresponds to the eigenfrequency of the injector. The power spectrum distribution shows large values as a whole at P_b=0.2 and 0.3 MPa. At Re=68000 the cavitation flows at P_b=0.2 and 0.3 MPa belong to the sheet cavitation and cloud cavitation flow regimes, respectively. In the sheet cavitation flow regime, the injection oscillation shows large value. However, in the cloud cavitation regime the injector oscillation depends on where the cavitation bubble collapses. At Re=68000 the cavitation bubbles collapse in the middle of the passage after the growth of the cavitation. This causes the large oscillation of the injector. At P_b=0.1 MPa the power spectrum shows small values. The cavitating flow in this case corresponds to the hydraulic flip. In this regime, since the liquid flow detaches the one side wall at the entrance and never reattaches again until injection, the injector oscillation is suppressed.

Figure 6 depicts conceptually the relationship between the injector oscillation and the Reynolds number. As the Reynolds number increases under the constant back pressure, the cavitating flow changes from the smooth flow to

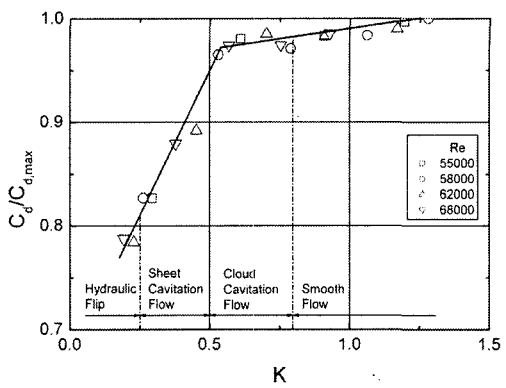

Fig.7 Relationship between discharge coefficient and K at constant flow rate

hydraulic flip. According to the changes of the cavitating flow pattern, the injector oscillation increases and has a maximum value in the sheet cavitation flow regime. Then, it decreases rapidly in the hydraulic flip regime.

The discharge coefficient is one of the important factors for the design of a rocket engine injector. As abovementioned, the cavitating flow pattern changes greatly by the back pressure and Reynolds number. And it is expected that the discharge coefficient changes according to the cavitating flow pattern. Figure 7 shows the relationship between the discharge coefficient and the cavitation number. The vertical axis indicates the discharge coefficient calculated from the following equation normalized by the maximum discharge coefficient:

$$C_d = \frac{Q}{A\sqrt{2\frac{P_i - P_b}{\rho}}} \tag{3}$$

where, Q, A and P_i indicate the volumetric flowrate of the water, cross sectional area of the orifice and the water injection pressure, respectively. The normalized discharge coefficient is nearly equal to one in the cloud cavitation flow and the smooth flow regimes. In the sheet cavitation flow and hydraulic flip regimes the normalized discharge coefficient decreases linearly with a decrease of the cavitation number. From the figure, it is clear that the effect of the Reynolds number on the discharge coefficient is small. Thus, the discharge coefficient of the nozzle is closely related with the pattern of the cavitating flow.

By the previous studies, the critical cavitation number, which classifies the cavitating flow pattern, varies according to the changing rate of the water flow rate. So, it is possible that the discharge coefficient varies according to the changing rate of the water flow rate. Figure 8 shows the time evolutions of the injection pressure and the discharge coefficient at P_b=0.1 MPa. As the injection pressure increases the water flow rate increases, and the cavitation number decreases. So, as the injection pressure increases the discharge coefficient decreases.

Figure 9 shows the relationships between the cavitation number and the discharge coefficient at P_b=0.1 MPa. In the figure, the discharge coefficient is almost

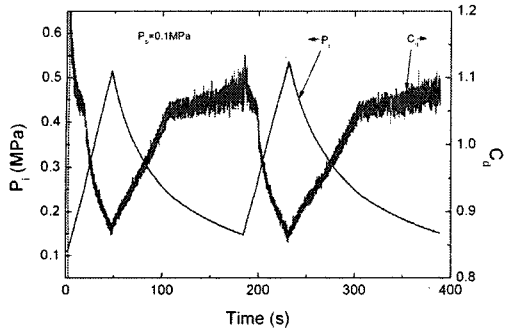

Fig.8 Time evolutions of injection pressure and discharge coefficient at P_b=0.1 MPa

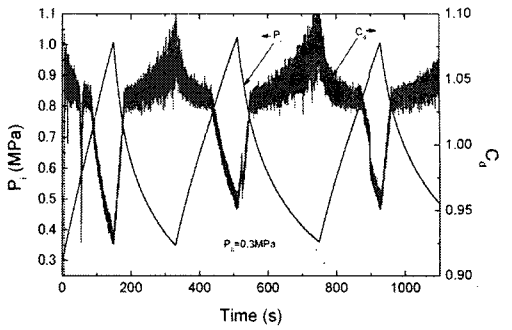

Fig.10 Time evolutions of injection pressure and discharge coefficient at P_b=0.3 MPa

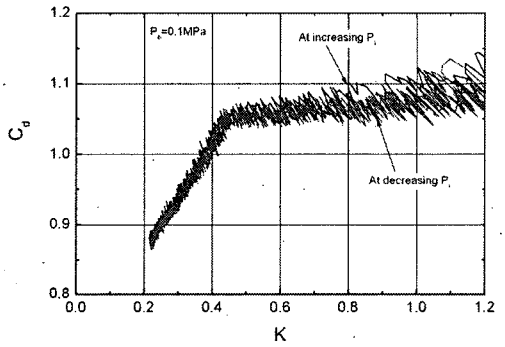

Fig.9 Relationships between cavitation number and discharge coefficient at P_b=0.1 MPa

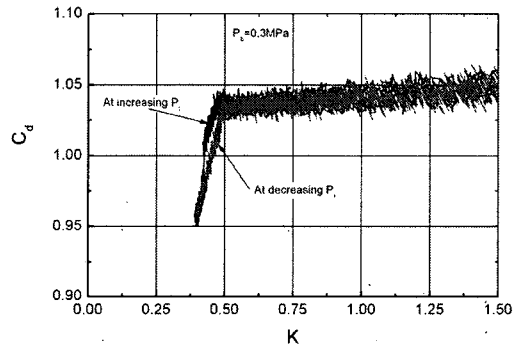

Fig.11 Relationships between cavitation number and discharge coefficient at P_b=0.3 MPa

constant when the cavitation number is greater than 0.45. At this condition, the cavitating flow belongs to the cloud cavitation or smooth flow regimes. And the oscillation of the injector is also small. When the cavitation number is smaller than 0.45, the discharge coefficient is proportional to the cavitation number. At this condition, the cavitating flow belongs to the sheet cavitation flow or the hydraulic flip regimes. In both cases of increasing and decreasing the water flow rate, the discharge coefficient changes along a same line as a function of the cavitation number.

Figures 10 and 11 show the time evolutions of the injection pressure and the discharge coefficient, and the relationships between the cavitation number and the discharge coefficient at P_b=0.3 MPa, respectively. At P_b=0.3 MPa, when the cavitation number decreases or increases, the discharge coefficient drops discontinuously. These phenomena occur randomly and their repeatability is not high. The discontinuous change of the discharge coefficient seems to be due to the transformation of the cavitating flow pattern. In this range of the cavitation number, the transformation of the cavitating flow from the sheet cavitation flow regime to the hydraulic flip regime at increasing the water flow rate or vise versa at decreasing the water flow rate occurs randomly. This random transformation of the cavitating flow causes the discontinuous drop of the discharge coefficient. In order to understand the mechanism of these phenomena, further investigation should be done.

Conclusions

In order to clarify the cavitating flow in the injector, the water injection experiments were carried out using the injector with the rectangular cross section and an orifice. And the relationship between the flow conditions and the cavitating flow patterns and the effects of the cavitating flow pattern on the atomization phenomena were investigated. As the experimental results, the cavitating flow patterns were classified using the cavitation number. The relationship between the cavitating flow pattern and the injector oscillation and the relationship between the cavitating flow pattern and the discharge coefficient were made clear. And it was made clear that the discontinuous change of the discharge coefficient occurs randomly at increasing or decreasing the cavitation number at the high back pressure.

References

(1) K.K.Kuo, ed., Recent Advances in Spray Combustion: Spray Atomization and Drop Burning Phenomena Vol.1, AIAA,1996.

(2) V.Yang and W.Anderson, ed., Liquid Rocket Engine Combustion Instability, AIAA, 1995.

(3) M.Arai, M.Shimizu and H.Hiroyasu, Break-up Length and Spray Formation Mechanism of a High Speed Liquid Jet, Proc. 4th ICLASS, pp. 177-184, 1988.

(4) H.Hiroyasu, Spray Breakup Mechanism from the Hole-type Nozzle and Its Applications, Atomization and Sprays, Vol.10, pp.511-527, 2000.